Optimization of the single quantum well CdHgTe/HgTe heterostructure parameters for the plasmon-phonons generation

© V.Ya. Aleshkin, A.O. Rudakov, A.A. Dubinov

Institute for Physics of Microstructures of the Russian Academy of Sciences,
603087 Afonino, Nizhny Novgorod region, Kstovsky district, Russia

E-mail: aleshkin@ipmras.ru

Received May 5, 2023
Revised June 5, 2023
Accepted June 5, 2023

Devoted to the choice of the optimal quantum well band gap for the generation of two-dimensional plasmon-phonons in CdHgTe/HgTe heterostructures. It is shown that the optimal effective band gap is a band gap that slightly exceeds the energy of a longitudinal optical phonon in the barrier.

Keywords: CdHgTe/HgTe heterostructures with quantum wells, generation of two-dimensional plasmon-phonons, optimal width of band gap.

DOI: 10.61011/SC.2023.04.56419.06k

1. Introduction

One of the urgent problems of semiconductor physics is the creation of a compact source of far-IR radiation. At present, the common radiation sources operating in this spectral area are quantum-cascade lasers [1]. Also, some of the devices that cover this spectral range are lead chalcogenide lasers. They operate at wavelengths up to $50\,\mu$m [2]. Due to the peculiarities of the material of these lasers, these lasers have not yet found commercial application. Another possible way to generate radiation in the spectral range of interest is the generation of two-dimensional plasmon-phonons in HgTe/CdHgTe heterostructures with narrow-gap quantum wells (QWs) [3], the technology of their growth by molecular-beam epitaxy is well developed at present [4,5].

The attractive aspects of plasmon-phonon generation are the large interband gain ($> 10^4\,\mathrm{cm}^{-1}$) [3] and the absence of the need for waveguides.

The Reststrahlen band of the QW material and the barrier in the considered structure overlap. In this case, the plasmon-phonon spectrum represents two branches — high-frequency and low-frequency, formed by interaction with optical phonons of the QW and the barrier. The low-frequency branch behaves proportionally to $\sqrt{q}$ at small wave vectors and tends to the frequency of the transverse optical phonon in the QW as the wave vector increases. The high-frequency branch starts from the longitudinal optical phonon energy in the barrier [6]. We will hereafter refer to such hybrid excitations as plasmon-phonons, following the terminology in Task 6.10 of book [7]. In structures to be considered, the role of the barrier is played by the solid solution $Cd_{0.7}Hg_{0.3}Te$. It has two longitudinal phonons (CdTe-like and HgTe-like). The maximum energy of the longitudinal optical phonon in $Cd_{0.7}Hg_{0.3}Te$ barriers is $\sim 20\,$meV (CdTe-like phonon) [8,9].

It is known that in the case when the band gap width becomes smaller than the frequency of the longitudinal optical phonon in the barrier and the QW, rapid recombination with the participation of the optical phonons becomes possible, preventing the creation of inverse population of the bands [10]. In order to exclude recombination involving phonons, it is necessary that the band gap width of the QW is larger than the energy of the longitudinal optical phonons in the barrier and the QW. Therefore, we will consider the QWs with parameters at which the band gap width is larger than the energy of the longitudinal optical phonon in the barrier and the QW. It is also necessary that the distance between the subbands of dimensional quantization of the valence band is larger than the band gap width. This will allow to exclude the absorption of plasmon-phonons in the range of interest, arising as a result of intersubband transitions of electrons in the valence band.

When inverse band population is created, plasmon-phonon gain becomes possible if the plasmon-phonon energy starts to exceed the value of the effective band gap width $E_{\mathrm{geff}}(q)$ [3]. By this value, we mean the minimum plasmon-phonon energy at a given wave vector q, possessing which it can be emitted at an interband electron transition. In the QWs whose band gap width is larger than the longitudinal optical phonon energy in the barrier, it is possible to realize the gain of plasmon-phonons of only the high-frequency branch. Therefore, we will not consider plasmon-phonons of the low-frequency branch in the following.

The plasmon-phonon dispersion law strongly depends on the concentration of non-equilibrium carriers. A decrease in concentration leads to a decrease in the phase velocity of the plasmon-phonon (i. e., for a given wave vector of the plasmon-phonon, its frequency decreases). When a certain concentration of non-equilibrium carriers is exceeded, the law of energy-momentum conservation at interband electron transitions with emission of plasmon-phonon [6] starts to be fulfilled. In conditions of inverse population, plasmon-phonon gain is possible at concentrations greater than the

indicated concentration. The carrier concentration, at which the plasmon-phonon gain begins, is called the threshold concentration. The reduction of the band gap width of the QW leads to the fact that the intersection of the plasmon-phonon dispersion curve and $E_{\text{geff}}(q)$ occurs at lower carrier concentrations. Thus, a decrease in the effective band gap width allows to reduce the concentration of non-equilibrium carriers, exceeding which becomes possible gain and generation of plasmon-phonons, in the presence of inverse population of the bands.

Earlier in the papers [11,12] various properties of plasmon-phonons in HgTe/CdHgTe structures with 5 nm wide QWs were studied. This corresponds to a band gap width of 35 meV. However, the issue of optimizing the structure parameters for plasmon-phonon generation has not been considered. In the present paper, we have made an attempt to fill this gap. We have shown that a decrease in the band gap width of the QW from 35 to 25 meV leads to a significant decrease in the threshold concentrations of carriers in structures with a single QW.

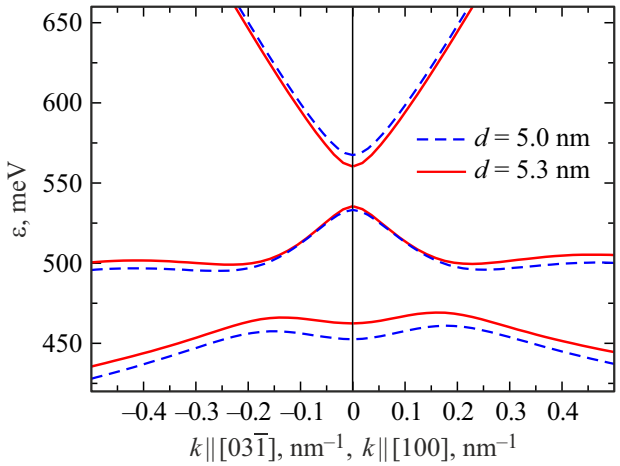

Figure 1. Electronic spectrum in HgTe QW surrounded by $Cd_{0.7}Hg_{0.3}Te$ barriers. The lattice temperature is 4.2 K. Blue dashed curves correspond to the spectrum in a 5 nm wide QW; red curves — in a 5.3 nm wide QW. (A color version of the figure is provided in the online version of the paper).

2. Calculation method

2.1. Plasmon-phonon spectrum

Consider a structure consisting of a single HgTe QW surrounded by solid solution barriers $Cd_xHg_{1-x}Te$ containing cadmium $x = 0.7$. Barriers of such composition are often used in such structures for the generation of electromagnetic waves of the range of interest [13,14]. We assume that a plasmon-phonon with wave vector $\mathbf{q}$ and frequency ω propagates in the QW plane. Plasmon-phonons, which can propagate in the considered structures, have a wavelength much larger compared to the QW width. Therefore, when studying the characteristics of plasmon-phonons, we will characterize the QW by two-dimensional polarizability, which is composed of the polarizability of free charge carriers, the polarizability due to the lattice vibrations of the QW and the electrons of the filled bands. In the framework of the random phase approximation, the expression for the two-dimensional polarizability of charge carriers, taking into account the collision frequency of non-equilibrium carriers, can be represented by the expression [6]:

$$\chi(\omega, \mathbf{q}) = \frac{e^2}{(2\pi)^2 q^2} \times \sum_{s,s'} \int d^2k \frac{\left[f_s(\mathbf{k}) + f_{s'}(\mathbf{k}+\mathbf{q})\right] \left| \int dz \psi^*_{\mathbf{k}+\mathbf{q},s'} \psi_{\mathbf{k},s} \right|}{\varepsilon_{s'}(\mathbf{k}+\mathbf{q}) - \varepsilon_s(\mathbf{k}) - \hbar\omega(\mathbf{q}) - i\hbar\nu}, \quad (1)$$

where e is the electron charge, $f(\mathbf{k})$ is the distribution function for non-equilibrium carriers, ν is the phase relaxation frequencies of non-diagonal elements of the density matrix, $\psi_{\mathbf{k}}$ is the electron wave function with wave vector $\mathbf{k}$, coordinate z is directed perpendicular to the QW plane. The summation is based on the indices s and s', which describe the subband number and spin states. Non-equilibrium carriers in the bands will be described by Fermi-Dirac statistics with effective temperature T_{eff}.

As can be seen from (1), to find the polarizability associated with the charge carriers, it is necessary to calculate the energies of the electrons and their wave functions. The Kane model was used to calculate them, taking into account deformation effects [15]. In calculating the energies and wave functions, we assume that the QW is grown in the (013) plane, and the lattice temperature is 4.2 K. We neglect the removal of spin degeneracy due to the absence of the inversion center and the lowering of symmetry at the heteroboundary. The influence of this effect on the characteristics of plasmon-phonons is small. It is possible to decrease the band gap width in the QW at the fixed barrier composition and lattice temperature by increasing the QW width. In this paper, we will compare the characteristics of plasmon-phonons in structures with QW widths of 5 and 5.3 nm. The calculated spectra of electrons in HgTe QWs with widths of 5 and 5.3 nm are shown in Fig. 1. The band gap width of the 5.3 nm wide QW is 25 meV. Note that this value is slightly larger than the energy of the longitudinal optical phonon in the barrier.

In calculating the polarizability by formula (1), we have taken into account 6 subbands: the first subband of the conduction band, the first and second subbands of the valence band (each subband is doubly degenerate in spin). The two-dimensional polarizability of the QW associated with phonons in the QW and filled band electrons is determined by the expression:

$$\chi_{\text{ph}}(\omega) = \kappa(\omega) d/4\pi,$$

where $\kappa(\omega)$ is the contribution to the dielectric constant of the QW due to the electrons of the filled bands and phonons in the QW; d is the width of the QW.

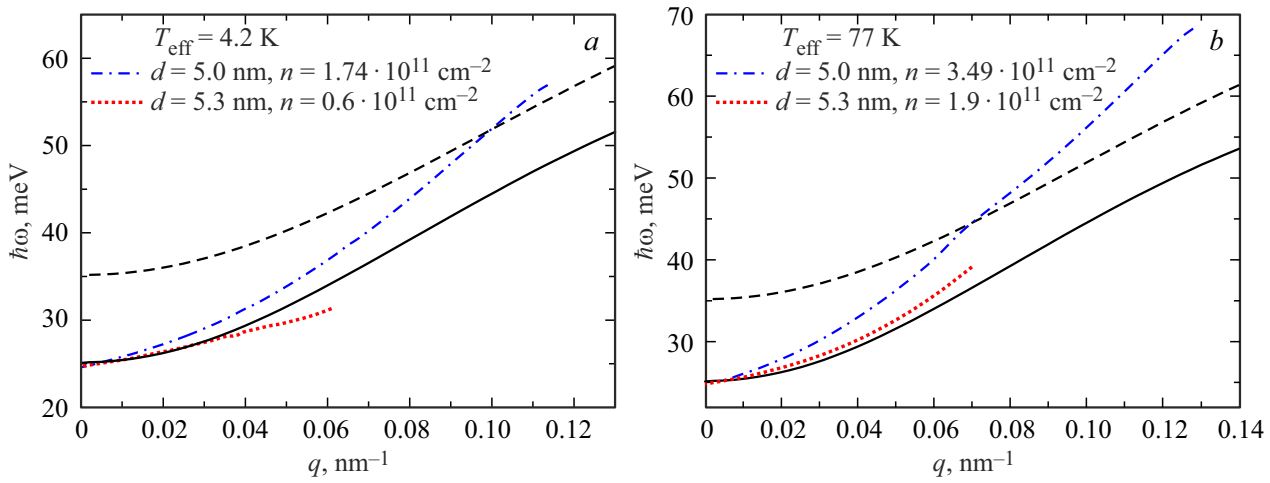

Figure 2. High-frequency branch plasmon-phonon spectra calculated for two effective temperatures of non-equilibrium carriers T_{eff}: panel *a* — corresponds to $T_{\text{eff}} = 4.2$ K, panel *b* — corresponds to $T_{\text{eff}} = 77$ K. The black dashed and solid lines show the $E_{\text{geff}}(q)$ dependences at QW widths of 5 and 5.3 nm, respectively.

Thus, the total polarizability of the QW has the form: $\chi_{\text{tot}}(\omega, \mathbf{q}) = \chi(\omega, \mathbf{q}) + \chi_{\text{ph}}(\omega)$. The contribution to the dielectric constant of HgTe due to lattice vibrations and filled band electrons in the case of low temperatures is determined by expression [16]:

$$\kappa(\omega) = \kappa_\infty + \frac{F\omega_{TO}^2}{\omega_{TO}^2 - \omega^2 - i\gamma\omega}, \qquad (2)$$

where F is the oscillator strength, ω_{TO} is the transverse optical phonon frequency in the QW, γ is the phonon attenuation frequency, κ_∞ is the dielectric permittivity associated with remote bands electrons. Electron transitions between the conduction band and the valence band do not contribute to the value of κ_∞. The frequency dependence of the dielectric constant of the $\kappa_B(\omega)$ barrier material is taken from the paper [17].

The formula (1) is obtained for the case, when the frequencies and wave vectors of the plasmon-phonon are real. However, if one considers the propagation of a plasmon-phonon with the real frequency ω in a medium with absorption, then the components of its wave vector are complex quantities. To make the wave vector of the plasmon-phonon propagating in the QW plane real, we consider the propagation of the plasmon-phonon in „ideal medium“. In this case, we artificially add a addition source to the QW to compensate for the absorption (gain) of the plasmon-phonon in the QW. We assume that the two-dimensional polarizability of this source is purely imaginary and opposite in sign to the imaginary part of the QW polarizability, i. e. $\chi_{QW}^{\text{source}} = -i\,\text{Im}\left[\chi_{\text{tot}}(\omega, \mathbf{q})\right]$. In addition, we introduce a source that compensates for the wave absorption in the barrier as well by adding an addition source to the barrier. Its bulk polarizability is also purely imaginary and opposite in sign to the imaginary part of the barrier polarizability, i. e $\chi_B^{\text{source}} = -i\,\text{Im}\left[\kappa_B(\omega)4\pi\right]$. Taking into account these statements, the total polarizability of the QW is determined by the expression $\chi_{\text{tot}}^{id.\text{med}}(\omega, \mathbf{q}) = \text{Re}\left[\chi_{\text{tot}}(\omega, \mathbf{q})\right]$, and the permittivity of the barriers is $\kappa_B^{id.\text{med}}(\omega) = \text{Re}\left[\kappa_B(\omega)\right]$. The dispersion equation for plasmon-phonons in a structure with one QW in „ideal medium“ has the following form

$$1 + 2\pi \frac{\text{Re}\left[\chi_{\text{tot}}(\omega, \mathbf{q})\right]}{\text{Re}\left[\kappa_B(\omega)\right]} Q = 0 \qquad (3)$$

where

$$Q^2 = q^2 - \frac{\omega^2}{c^2}\,\text{Re}\left[\kappa_B(\omega)\right].$$

The question arises as to how fair this approximation is. To analyze the accuracy of this approximation, we can compare the solutions obtained from equation (3) and the exact solutions of equation (3) obtained in the absence of spatial dispersion of polarizability. These solutions agree well in the case when $\text{Re}\,[q] > \text{Im}\,[q]$. Solutions of the dispersion equation (3) for high-frequency plasmon-phonon modes in the considered structures are given in Fig. 2 at two effective temperatures of non-equilibrium carriers. When calculating the plasmon-phonon spectra, we neglected the equilibrium concentration of electrons and holes in the bands and assumed the concentration of non-equilibrium electrons to be equal to the concentration of non-equilibrium holes. The concentration of non-equilibrium carriers used in the calculation of the plasmon-phonon spectra is slightly higher than the threshold concentration (i. e., such concentrations were chosen whose decrease by 10^{10} cm^{-2} would lead to no gain).

It can be seen from Fig. 2, that QW width increase from 5 to 5.3 nm leads to a decrease in the effective band gap width $E_{\text{geff}}(q)$. A decrease in $E_{\text{geff}}(q)$ leads to a decrease in the threshold concentration of non-equilibrium carriers. Although the plasmon-phonon phase velocity ($v_{\text{ph}} = \omega/q$) becomes lower with the decreasing carrier concentration, the intersection with the $E_{\text{geff}}(q)$ dependence

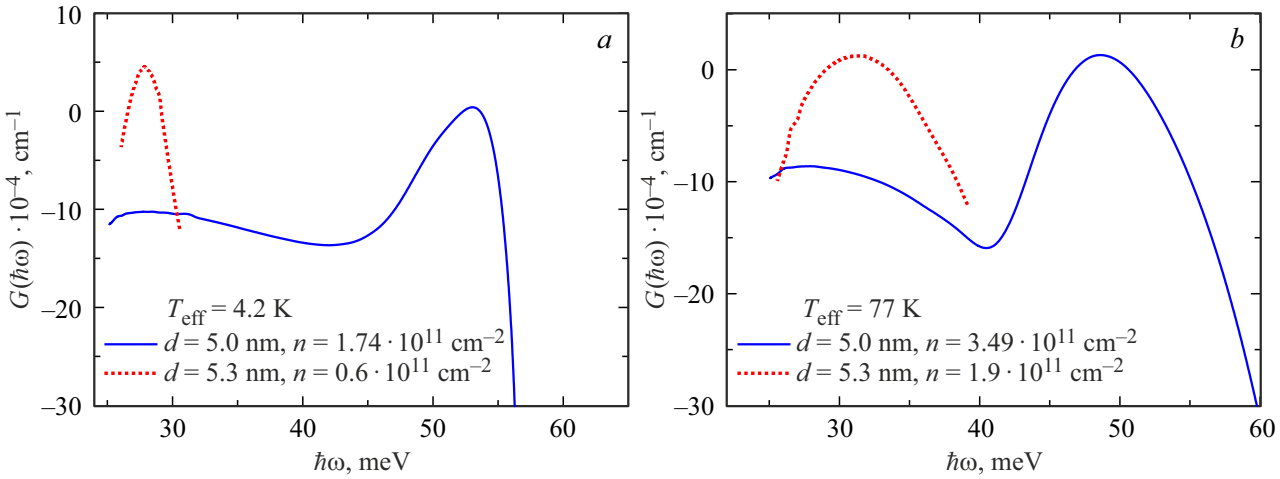

Figure 3. Plasmon-phonon gain spectra calculated for two effective temperatures of non-equilibrium carriers in structures with QW widths of 5 and 5.3 nm: *a* — corresponds to $T_{\text{eff}} = 4.2$ K, *b* —corresponds to $T_{\text{eff}} = 77$ K.

occurs at smaller plasmon-phonon wave vectors (red curve in Fig. 2). A decrease in the threshold concentration of non-equilibrium carriers leads to the fact that the generation of plasmon-phonons with lower energies and wave vectors at lower concentrations of non-equilibrium carriers is possible in a narrower band gap QW. Due to the fact that the high-frequency plasmon-phonon branch of the spectrum begins at a finite frequency, plasmon-phonons with small wave vectors have a greater phase velocity (i. e., the refraction index of these waves is smaller than the refraction index of waves that can be amplified in a wide-band structure).

One of the problems complicating the detection of plasmon-phonons is the emission of this wave from the structure. The reflectance of these waves from the edge of the structure is large because of the large effective refraction index of the plasmon-phonon. The reflectance of plasmon-phonons from the edge of the structure rises with the effective refraction index growth.

In the structure with a 5 nm wide QW, the effective refraction index at the point of intersection of the plasmon dispersion curve with $E_{\text{geff}}(q)$ is 395, and in the structure with a QW with a width of 5.3 nm is 64. Thus, the plasmons reflectance from the narrow-gap structure boundary with air is smaller than the same value for the wide-band structure. One of the ways to lead plasmon-phonons out of the structure is to lead them out using a lattice created on the surface of the structure parallel to the QW plane. The lattice is necessary to fulfil the law of conservation of momentum plasmon emission [18]. The period of such a lattice is proportional to $2\pi/q$. To emit plasmon-phonons with small wave vectors, a lattice with a large period is required. For example, to emit plasmon-phonons from a structure with a 5.3 nm wide QW, a lattice with a period $\sim 0.6\,\mu$m is needed, while to emit plasmon from a structure with a 5 nm wide QW, a lattice with a period $\sim 0.06\,\mu$m is needed, which is more difficult to realize.

2.2. Plasmon-phonon gain

The plasmon-phonon absorption coefficient is the ratio of the difference between the absorbed and emitted power densities during plasmon-phonon propagation in the structure to the plasmon-phonon energy flux per unit length. Power absorption occurs due to Drude losses, phonon losses in the QW and barriers, as a result of intersubband electron transitions in the valence band, interband electron transitions from the valence band to the conduction band, and Landau damping (intraband absorption of plasmons by electrons). The power release is due to electron transitions from the conduction band to the valence band.

The total power density absorbed by the QW is equal to:

$$P_{QW}(\omega, \mathbf{q}) = 2|E_0|^2\omega\,\mathrm{Im}\left[\chi_{\text{tot}}(\omega, \mathbf{q})\right], \tag{4}$$

where E_0 is the magnitude of the electric field component lying in the QW plane.

The power absorbed by a unit area of the barrier due to phonon losses is equal to:

$$P_B(\omega) = 2|E_0|^2\omega\,\mathrm{Im}\left[\frac{\kappa_B(\omega)}{4\pi Q}\left(1 + q^2/Q^2\right)\right]. \tag{5}$$

Using the expression for the Pointing vector, an expression for the plasmon-phonon energy flux in a structure with a single QW can be obtained:

$$I(\omega, \mathbf{q}) = \frac{\omega q}{2\pi Q^3}\,\mathrm{Re}\left[\kappa_B(\omega)\right]|E_0|^2. \tag{6}$$

Dividing by (6) the sum of (4) and (5), we obtain an expression for the plasmon-phonon absorption coefficient:

$$\alpha(\omega, \mathbf{q}) = \frac{4\pi Q^3}{q\,\mathrm{Re}\left[\kappa_B(\omega)\right]}\,\mathrm{Im}\left[\chi_{\text{tot}}(\omega, \mathbf{q}) + \frac{\kappa_B(\omega)}{4\pi Q}\left(1 + \frac{q^2}{Q^2}\right)\right]. \tag{7}$$

In the frequency range where this value is negative, the plasmon-phonon is amplified. It is more convenient to

consider the value $G(\omega, \mathbf{q}) = -\alpha(\omega, \mathbf{q})$, called the mode gain.

The dependences of the gain on frequency calculated using formula (7) are shown in Fig. 3. The concentrations of non-equilibrium carriers, at which the plasmon-phonon mode gain spectra shown in Fig. 3 are found, are slightly higher than the threshold ones and equal to QW 5 nm $n = 1.74 \cdot 10^{11}\,\mathrm{cm}^{-2}$ at $T_{\mathrm{eff}} = 4.2\,\mathrm{K}$ and $n = 3.49 \cdot 10^{11}\,\mathrm{cm}^{-2}$ at $T_{\mathrm{eff}} = 77\,\mathrm{K}$. For the structure with a 5.3 nm QW width, the concentrations are $n = 0.6 \cdot 10^{11}\,\mathrm{cm}^{-2}$ at $T_{\mathrm{eff}} = 4.2\,\mathrm{K}$ and $n = 1.9 \cdot 10^{11}\,\mathrm{cm}^{-2}$ at $T_{\mathrm{eff}} = 77\,\mathrm{K}$.

It can be seen from Fig. 3, when the effective band gap width is reduced from 35 to 25 meV, it becomes possible to gain longer wavelength plasmon-phonons. In addition, the threshold concentrations of non-equilibrium carriers decrease significantly with increasing the width of the QW.

An increase in T_{eff} leads to an increase in threshold concentration. This can be explained by the fact that the electron population of states above the Fermi quasi-levels will increase as the effective temperature of non-equilibrium carriers increases. Due to the non-parabolicity of the electron spectrum, the density of electron states increases with increasing electron energy in the conduction band and decreases in the valence band. This will lead to a decrease in the Fermi quasi-level difference with increasing T_{eff} at a fixed carrier concentration. Consequently, the number of interband electron transitions contributing to the plasmon-phonon enhancement will decrease. The same consequence leads to a decrease in the population of electron states under the Fermi quasi-levels with increasing effective temperature of non-equilibrium carriers. In addition, an increase in the effective temperature of non-equilibrium carriers will lead to an increase in the Landau damping. This is explained by the fact that at the temperature increase above the Fermi quasi-level in the conduction band, there will be more electrons able to participate in the process of intraband absorption of plasmon-phonons. Therefore, the threshold concentration increases with increasing temperature.

3. Conclusion

In paper, we have compared the plasmon-phonon characteristics of high-frequency branch plasmons in heterostructures with quantum wells with band gap widths of 35 and 25 meV grown on the plane (013). It is shown that a reduction of the band gap width to 25 meV leads to a threefold decrease in the threshold concentration of non-equilibrium carriers at the effective temperature of non-equilibrium carriers at 4.2 K and a twofold at 77 K. High-frequency branch plasmon-phonons with small wave vectors have a smaller reflectance from the edge of the structure compared to plasmon-phonons with large wave vectors. An increase in the effective temperature of non-equilibrium carriers leads to an increase in the threshold concentration.

Note that the spectrum of plasmon-phonons in the considered structures is mainly determined by electrons, since they have greater mobility compared to holes. The electron spectra in the conduction band of the structures grown on the (001) and (013) planes and having the same band gap width differ slightly. Therefore, the conclusions obtained in this paper about the optimal band gap width ~ 25 meV for plasmon-phonon generation are also valid for structures grown on the plane (001).

Funding

This study was supported by the Russian Science Foundation (grant No. 22-12-00310).

Conflict of interest

The authors declare that they have no conflict of interest.

References

[1] M.S. Vitiello, G. Scalari, B. Williams, P. De Natale. Opt. Express, **23**, 5167 (2015).
[2] K.V. Maremyanin, A.V. Ikonnikov, L.S. Bovkun, V.V. Rumyantsev, E.G. Chizhevskii, I.I. Zasavitskii, V.I. Gavrilenko. Semiconductors, **52**, 1590 (2018).
[3] K. Kapralov, G. Alymov, D. Svintsov, A. Dubinov. J. Phys.: Condens. Matter, **32**, 065301 (2019).
[4] S. Dvoretsky, N. Mikhailov, Y. Sidorov, V. Shvets, S. Danilov, B. Wittman, S. Ganichev. J. Electron. Mater., **39**, 918 (2010).
[5] N. Mikhailov, R. Smirnov, S. Dvoretsky, V. Sidorov, Y.G. Sidorov, V. Shvets, E. Spesivtsev, S. Rykhlitski. Int. J. Nanotechnol., **3**, 120 (2006).
[6] V.Ya. Aleshkin, A.A. Dubinov, V.I. Gavrilenko, F. Teppe. J. Optics, **23**, 115001 (2021).
[7] Yu. Peter, M. Kardona. Fundamentals of semiconductors: physics and materials properties. Springer Science & Business Media, 2010.
[8] J. Baars, F. Sorger. Solid State Commun., **10**, 875 (1972)
[9] D.N. Talwar, M. Vandevyver. J. Appl. Phys., **56**, 1601 (1984)
[10] V.Ya. Aleshkin, A.A. Dubinov, V.I. Gavrilenko, S.G. Pavlov, H.-W. Hubers. Physics of Solid State, **64**, 168 (2022).
[11] V.Ya. Aleshkin, G. Alymov, A.A. Dubinov, V.I. Gavrilenko, F. Teppe, J. Phys. Commun., **4**, 115012 (2020).
[12] V.Ya. Aleshkin, A.A. Dubinov, V.I. Gavrilenko, F. Teppe. Appl. Optics, **60**, 8991 (2021).
[13] S.V. Morozov, V.V. Rumyantsev, M.S. Zholudev, A.A. Dubinov, V.Ya. Aleshkin, V.V. Utochkin, M.A. Fadeev, K.E. Kudryavtsev, N.N. Mikhailov, S.A. Dvoretskii, V.I. Gavrilenko, F. Teppe. ACS Photonics, **8**, 3526 (2021).
[14] V.V. Rumyantsev, A.A. Dubinov, V.V. Utochkin, M.A. Fadeev, V.Ya. Aleshkin, A.A. Razova, N.N. Mikhailov, S.A. Dvoretsky, V.I. Gavrilenko, S.V. Morozov. Appl. Phys. Lett., **121**, 182103 (2022).
[15] M. Zholudev, F. Teppe, M. Orlita, C. Consejo, J. Torres, N. Dyakonova, M. Czapkiewicz, J. Wróbel, G. Grabecki, N. Mikhailov, S. Dvoretskii. Phys. Rev. B, **86**, 205420 (2012).
[16] M. Grynberg, R. Le Toullec, M. Balkanski. Phys. Rev. B, **9**, 517 (1974).
[17] J. Polit. Bull. Polish Acad. Sci. Techn. Sci., **59**, 331 (2011).
[18] G. Fasol, N. Mestres, H.P. Hughes, A. Fischer, K. Ploog. Phys. Rev. Lett., **56**, 2517 (1986).

Translated by Y.Deineka